

Electrochemical deposition of p-type CuSCN in porous n-type TiO₂ films

W.B. Wu^a, Z.G. Jin^b, G.D. Hu^{a,*}, S.J. Bu^c

^a School of Materials Science and Engineering, Jinan University, Shandong 250022, PR China

^b Key Laboratory for Advanced Ceramics and Machining Technology of Ministry of Education, Tianjin University, Tianjin 300072, PR China

^c School of Materials Science and Engineering, Tianjin 300130, Hebei University of Technology, PR China

Received 4 November 2006; received in revised form 8 January 2007; accepted 18 January 2007

Available online 30 January 2007

Abstract

We present an energy band model and a method for filling p-type CuSCN in n-type porous TiO₂ film. The energy band model is based on the interface energy levels between TiO₂/CuSCN heterojunction and the aqueous electrolyte. The whole deposition process is divided into three stages: the uniform nucleation on the internal surface at positive potential, the crystal growth with the cathodic potential shifting negatively and the thermal activated growth at constant potential. This was demonstrated by the electrochemical experiment combining the hydrothermal process. It was found that the obtained TiO₂/CuSCN heterojunction exhibited good rectification characteristics, indicating that an intimate electrical contact was formed between the large internal surface of TiO₂ film and CuSCN. This novel hydrothermal-electrochemical method may be valuable for fabricating extremely thin absorber (eta)-solar cells and other semiconductor devices.

© 2007 Elsevier Ltd. All rights reserved.

Keywords: CuSCN; Porous TiO₂ film; Energy band model; Hydrothermal-electrochemical method; Eta-solar cell

1. Introduction

Semiconductor growth on highly structured and porous substrates is of interest for a range of electrical, chemical and catalytic applications. One typical example is the extremely thin absorber (eta)-solar cell, mainly consisting of a porous n-type window layer, an inorganic eta layer, and a wide-band-gap p-type layer. Highly structural substrates, such as porous TiO₂ and ZnO nanowire films, are used for windows layer to enhance light trap and improve the separation efficiency of the excited carriers [1–4]. Narrow-band-gap materials, CdTe [5], HgCdTe [6], CuInS₂ [7], CdSe [8], etc., are used for absorbers. Among the p-type layer materials, CuSCN is considered the most promising for its stability and technical feasibility in filling pores [9,10].

Conformal deposition of eta layer and p-type layer in pores of substrate is crucial for obtaining high energy efficiency. Although some advanced deposition techniques, MBE, MCVD, PLD and ALD, are the desirable methods for plane substrates, the problem of non-uniform deposition arises for porous substrates due to the shadow effect [3,4]. Many efforts have been made to resolve the problems [2,3,11–13]. Among these, elec-

trochemical deposition (ED) is considered one standard method for coating complex shapes [14]. For example, it has been a preferred technique for depositing metallic copper in the complex damascene patterns in integrated circuits [15]. The deposition of CuSCN in porous substrates with the ED method has been reported [7,12]. It has ever been thought that the organic electrochemical deposition solution is better than the aqueous solution because the aqueous solution is unstable as well as unsuitable for obtaining fine structure [16]. However, in our previous work, a stable aqueous solution was prepared. In addition, the fine CuSCN film was deposited on ITO glass from the aqueous solution by ED and the formation mechanisms was also discussed [17]. Further, in the present study, we investigated the deposition of CuSCN in porous TiO₂. A three-stage energetic model was proposed for filling CuSCN in pores of TiO₂ substrate. Furthermore, this was confirmed by a hydrothermal-electrochemical experiment.

2. Experimental

2.1. Porous TiO₂ electrode formation

The porous TiO₂ film was deposited directly on conductive indium tin oxide coated glass (ITO, 10 Ω/□) by a sol-gel dip-

* Corresponding author. Tel.: +86 53185175201; fax: +86 53182767915.
E-mail address: mse_hugd@ujn.edu.cn (G.D. Hu).

coating technology [18]. In details, the precursor sol solution was obtained by following steps: dissolve 0.5 M $\text{Ti}(\text{OC}_4\text{H}_9)_4$ and 1 M diethanolamine (DEA) in ethanol, hydrolyze and add 20 g/L polyethylene glycol (PEG, molecular weight 1000) under magnetic stirring. The precursor sol film was dip coated on ITO glass. The porous TiO_2 electrode was obtained after the precursor film was aged at 100°C for 10 min and calcined at 550°C for 1 h in air.

2.2. Electrochemical deposition of CuSCN

The CuSCN films were deposited on ITO glass and the as-prepared TiO_2 electrode by the electrochemical method, respectively. The stable aqueous electrolyte, with 0.06 M CuSO_4 , 0.03 M KSCN and 0.06 M EDTA, was prepared based on our previous study [17]. The pH value was adjusted to 2–2.6 with sulphuric acid (H_2SO_4). Electrochemical deposition and measurement were carried out on the LK2005 electrochemical workstation (Tianjin, China). The normal three-electrode electrochemical cell was placed in a hydrothermal bath. The reference electrode and the counter electrode were Ag/AgCl and Pt, respectively. Potentials mentioned later are all respect to Ag/AgCl electrode. A thin Au layer was sputtered on the obtained heterojunction film for subsequent current–voltage test.

2.3. Characterization

Scanning electron microscope (SEM) images were taken on a PHILIPS XL-30 environment scanning electron microanalyzer. N_2 adsorption was measured on a Quanta-chrome Nova 2000 specific area instruments. The Mott–Schottky plots and the I – V plot were measured on the advanced electrochemical system (PARSTAT 2263, EG&G).

3. Results and discussion

3.1. Structural and electrochemical characteristics of TiO_2 and CuSCN films

To elucidate the interface energy levels, the structural and the electrochemical properties of TiO_2 electrode and CuSCN film were characterized, respectively.

Fig. 1a and b shows the typical morphologies of the surface and the cross-section of the as-prepared porous TiO_2 film. The TiO_2 film exhibits a highly interpenetrated porous structure with pore size of 200–300 nm and the thickness of $\sim 1\ \mu\text{m}$. The surface enlargement factor is over 10 for a BET surface area of $72\ \text{m}^2\ \text{g}^{-1}$ [18]. This unique structure is suitable for eta-solar cells [19].

The flat band potential (E_{fb}) of TiO_2 electrode and CuSCN film can be obtained from the Mott–Schottky plots according to the M–S equation: $1/(C_{\text{sc}})^2 \propto E - E_{\text{fb}} - kT/e$, where C is the differential capacitance of the space charge layer. The measuring aqueous electrolyte, with 0.2 M KSCN and a pH value of 2.1, is similar to the electrochemical deposition solution [17]. E_{fb} was obtained by extrapolating the linear part to the potential axis where $1/(C_{\text{sc}})^2 = 0$. The linear part in M–S plot suggests that the

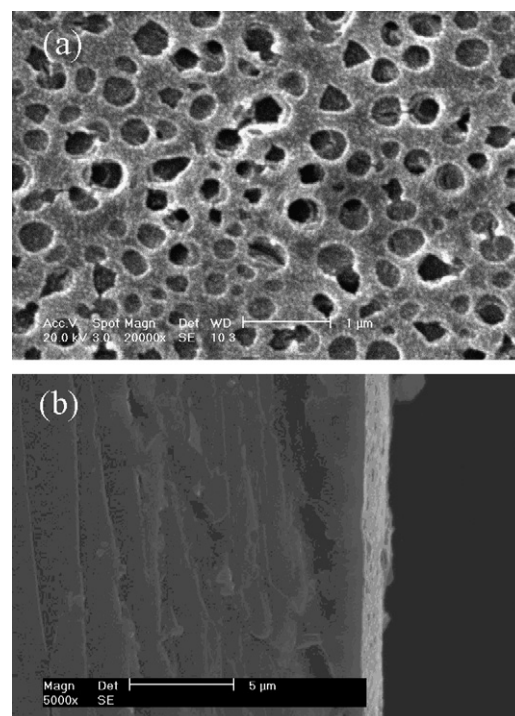


Fig. 1. SEM photographs of: (a) the surface and (b) the cross-section of as-prepared porous TiO_2 film.

TiO_2 particles are interconnected and partly fused together rather than individually dispersed as reported by Cao and Hagfeldt [19,20]. The E_{fb} of $-0.07\ \text{eV}$ accords with the surface states' Fermi level (E_{fs}) of TiO_2 nanoparticles but is obvious lower than the E_c ($0.51\ \text{eV}$) of nanocrystalline anatase TiO_2 , implying that the E_{fs} in the band gap will provide the dominant pathway for electron transfer between TiO_2 nanoparticles and acceptor species in electrolyte solution [21]. From Fig. 2b, it is found that CuSCN film is p-type and the E_{fb} is about $-0.41\ \text{eV}$, consistent with that from O'Regan et al. [8]. Since the E_{fs} of TiO_2 electrode is higher than the E_{fb} of CuSCN, electrons will transfer from TiO_2 to CuSCN when the cathodic potential is more negative than the E_{fb} of CuSCN.

3.2. Energy band model for deposition of CuSCN in porous TiO_2 film

The energy band model is discussed based on the above energy levels and the E_{redox} of the electrolyte. As well known, owing to the band-edge pinning effect, a space charge layer can be formed at the interface when a semiconductor is in direct contact with an electrolyte. If the E_{fb} or E_{fs} is higher than E_{redox} , electrons in solid will transfer to the acceptor species in electrolyte, resulting in a depletion layer in the semiconductor. Otherwise, an accumulation layer will be formed.

For the case of the interface between TiO_2 /CuSCN heterojunction and the electrolyte, the distribution of the energy levels is much more complex, as shown in Fig. 3. If the CuSCN side is thick enough, four regions will be formed. In region I, the quasi-Fermi level for holes (E_{fp}) extends to n-type side. The width decreases with the negative shift of the cathodic potential.

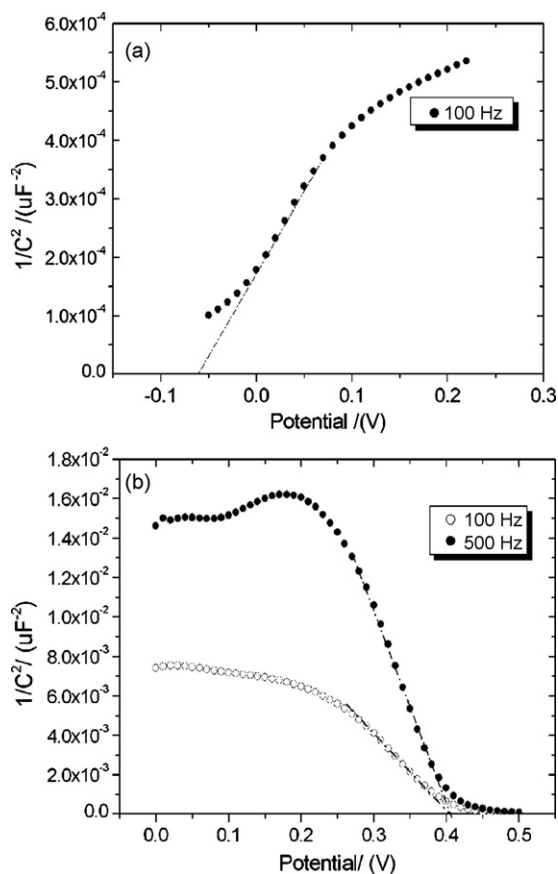


Fig. 2. Mott-Schottky plots of: (a) porous TiO_2 films and (b) CuSCN films in 0.2 M KSCN aqueous solution, pH 2.1. The measuring frequency is 100 and 500 Hz.

In region II, the quasi-Fermi level for electrons (E_{fn}) in p-type side is higher than both of the E_{redox} and the E_{fp} . In region III, the E_{fn} is located between the E_{redox} and the E_{fp} and descends toward the electrolyte. As for region IV, only the E_{fp} is left. The widths of regions II and III will increase with the negative shift of the cathodic potential. According to our previous study, the deposition reaction in regions III and IV is predominated by

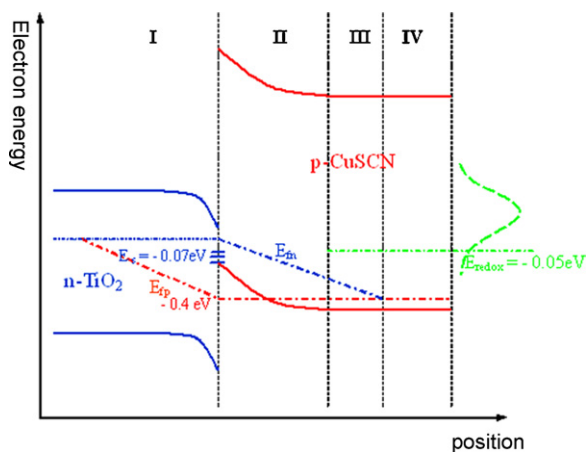


Fig. 3. Band edges and quasi-Fermi levels for electrons and holes of $\text{CuSCN}/\text{TiO}_2$ heterojunction at negative bias with respect to the equilibrium potential.

the thermal activation of the surface states ($\text{Cu}^{\text{II}}(\text{SCN})_x$) or the acceptor species (Cu^{II}), because the thermal fluctuation of the surface state or the acceptor species levels (0.5 eV at 55 °C) is much larger than the thermal energy ($kT \approx 0.03$ eV at 55 °C) of electrons and holes in CuSCN [17].

According to the above energy model, we propose a three-stage process for the deposition of CuSCN . In the initial stage, TiO_2 electrode is in direct contact with the electrolyte. For conformal deposition on the internal surface of the TiO_2 electrode, small CuSCN crystalline particles are required. To ensure the size of nuclei as small as possible, the initial deposition potential must be set lower than the E_{redox} . Thus, once a thin layer of p-type CuSCN nuclei is formed on TiO_2 , the electrons flowing will be inhibited since the deposition potential is a backward bias for the just formed junction. Then, the crystal growth is prevented. The subsequent transfer of electrons will take place only on the bare TiO_2 . Consequently, the internal surface will be completely covered with a thin CuSCN nuclei layer. In addition, to avoid the crystal growth by the thermal activation of the acceptor species or the surface states, the deposition must be performed at a temperature lower than 10 °C.

In stage II, corresponding to region II, the formed CuSCN nuclei will grow by electrons injection through the E_{fn} extending to CuSCN as the cathodic potential shifts negatively. The final potential must be under -0.5 V. Otherwise, Cu-rich compounds or metallic copper will be formed [17]. The process is terminated until the thickness of CuSCN reaches the maximum width of region II at the constant potential -0.5 V, when the deposition current is constant and the very small current is resulted due to the thermal activation.

In stage III, combining the above discussion about regions III and IV, it can be inferred that CuSCN crystals grow only by the thermal activation of the acceptor species or the surface states. This can be realized by elevating the deposition temperature.

3.3. Deposition and characteristic of CuSCN in porous TiO_2 electrode

According to above discussion, we designed a hydrothermal-electrochemical process. Firstly, the deposition was performed at +0.1 V and 10 °C and kept for several minutes to produce a thin CuSCN nuclei layer. Then, the deposition potential was scanned from +0.1 to -0.5 V by a small step of 1 mV/s to deposit CuSCN layer by layer. The procedure was maintained at the constant potential (-0.5 V) until the deposition current was constant. In the following stage, the temperature was elevated to 45 °C by a step of 2 °C/min and held for 15 min. Then, a $\text{TiO}_2/\text{CuSCN}$ heterojunction film was resulted. The current and temperature plots against time during the deposition are shown in Fig. 4. It can be found that the current trend is well consistent with the above discussion. Because the three deposition stages are realized by five segregated steps, the current density increases sharply at the very beginning of every step, which is due to the charging of the double charge layer. In the stage V, the current fluctuates with the fluctuation of the temperature. The growth rate of the CuSCN crystal is very correlative with the temperature for the

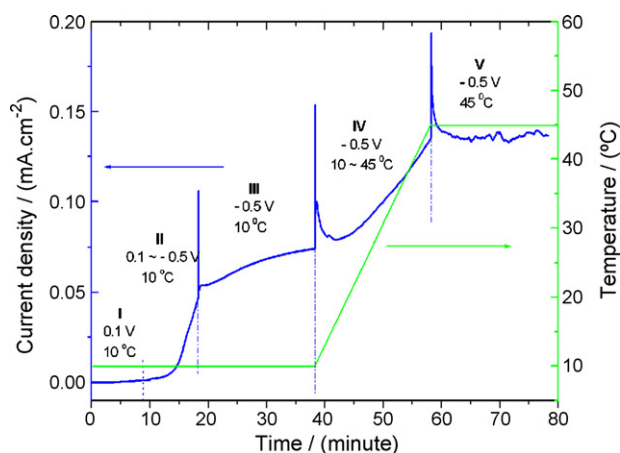


Fig. 4. Plots of current and temperature against time at three deposition stages. The whole deposition is divided into five segregated steps.

current density varies largely with the temperature. It can be predicted that the junction quality can be further improved if the deposition is performed at lower temperature close to 0 °C.

Fig. 5a and b shows the SEM photographs of the surface and the cross-section of the TiO₂/CuSCN heterojunction. It is found that, in addition to the dense CuSCN in pores, a pure CuSCN layer with the thickness of ~1 μm is produced on the surface. The CuSCN layer is dense besides of several large particles on top surface, which may originate from the leaking current due to the polycrystalline structure. Our TiO₂/CuSCN heterojunction film is largely improved compared to that from the organic electrolyte [22].

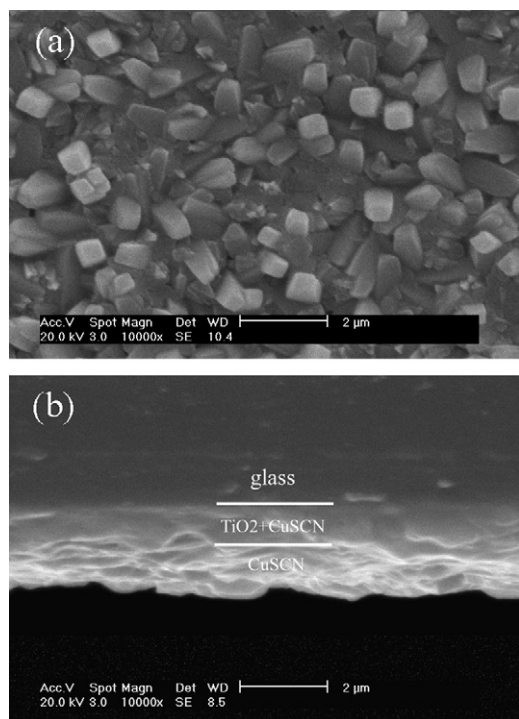


Fig. 5. SEM photographs of: (a) the surface and (b) cross-section of TiO₂/CuSCN heterojunction deposited by the potential scanning from 0.1 to -0.5 V, followed by elevating temperature.

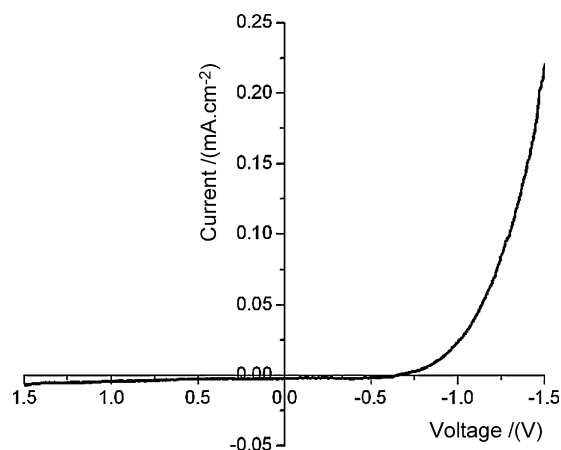


Fig. 6. Current–voltage characteristic of TiO₂/CuSCN heterojunction.

Fig. 6 shows the typical current–voltage curve of the heterojunction film. The heterojunction shows good rectifying behavior with the rectification ratio of ~33, the reverse saturation current of $\sim 6 \times 10^{-3}$ mA/cm², and the series resistance of $\sim 1 \times 10^3 \Omega$. The series resistance can be substantially reduced by adjusting the thickness of CuSCN and TiO₂ layers more carefully. Our results suggest that a good electronic contact is formed between the large area TiO₂ and CuSCN layer.

4. Conclusions

An energy band model for depositing TiO₂/CuSCN heterojunction film has been established based on the interface energy levels between the p–n heterojunction and the aqueous electrolyte. According to the model, we propose a three-stage deposition procedure: the uniform nucleation on pore walls at positive potential, the crystal growth at negative potential and the thermal activated growth at constant potential. This is further confirmed by a hydrothermal-electrochemical process. The as-prepared TiO₂/CuSCN heterojunction exhibits good rectification characteristics. The rectification ratio is ~33 and the reverse saturation current is $\sim 6 \times 10^{-3}$ mA/cm². The results indicate that a good electric contact has been formed between large area TiO₂ and CuSCN. The hydrothermal-electrochemical technique has potential applications in eta-solar cells and other p–n heterojunction systems.

References

- [1] R. Könenkamp, L. Dloczik, K. Ernst, C. Olesch, *Physica E* 14 (2002) 219.
- [2] R. Könenkamp, K. Ernst, C.H. Fisher, M.C. Lux-Steiner, C. Rost, *Phys. Status Solidi A* 182 (2000) 151.
- [3] R. Tena-Zaera, M.A. Ryan, A. Katty, G. Hodes, S. Bastide, C. Lévy-Clément, *C. R. Chim.* 9 (2006) 717.
- [4] C. Lévy-Clément, A. Katty, S. Bastide, F. Zenia, I. Mora, V. Muñoz-Sanjosé, *Physica E* 14 (2002) 229.
- [5] R. Tena-Zaera, A. Katty, S. Bastide, C. Lévy-Clément, B. O'Regan, V. Muñoz-Sanjosé, *Thin Solid Films* 486 (2005) 372.
- [6] K. Ernsta, I. Siebera, M. Neumann-Spallartb, M.-Ch. Lux-Steinera, R. Könenkamp, *Thin Solid Films* 361–362 (2000) 213.
- [7] R.B. Belaidi, L. Dloczik, K. Ernst, M.C. Lux Steiner, R. Könenkamp, *Thin Solid Films* 431–432 (2003) 488.

- [8] A. Hagfeldt, U. Björkstén, M. Grätzel, *J. Phys. Chem.* 100 (1996) 8045.
- [9] B. O'Regan, T. Daniel, D.T. Schwartz, *Adv. Mater.* 12 (2000) 1263.
- [10] B. O'Regan, F. Lenzmann, R. Muis, J. Wienke, *J. Chem. Mater.* 14 (2003) 5023.
- [11] G.R.R.A. Kumara, A. Konno, G.K.R. Senadeera, P.V.V. Jayaweera, D.B.R.A. De Silva, K. Tennakone, *Sol. Energy Mater. Sol. Cells* 69 (2001) 195.
- [12] C. Rost, I. Sieber, S. Siebentritt, M.C. Lux-Steiner, R. Könenkampa, *Appl. Lett. Phys.* 75 (1999) 692.
- [13] K.E. Kaiser, C.H. Fischer, M.C. Lux Steiner, R. Könenkamp, *Sol. Energy Mater. Sol. Cells* 67 (2001) 89.
- [14] B.R. Sankapal, E. Goncalves, A. Ennaoui, M.Ch. Lux-Steiner, *Thin Solid Films* 451–452 (2004) 128.
- [15] P.C. Andricacos, et al., *IBM J. Res. Dev.* 42 (1998) 567.
- [16] K. Tennakone, A.R. Kummarasinghe, P.M. Sirimanne, G.R.R.A. Kumara, *Thin Solid Films* 261 (1995) 307.
- [17] W.B. Wu, Z.G. Jin, Z. Hua, Y.N. Fu, J.J. Qiu, *Electrochim. Acta* 50 (2005) 2343.
- [18] S.J. Bu, Z.G. Jin, X.X. Liu, L.R. Yang, Z.J. Cheng, *Mater. Chem. Phys.* 88 (2004) 273.
- [19] A. Hagfeldt, U. Björkstén, M. Grätzel, *J. Phys. Chem.* 100 (1996) 8045.
- [20] F. Cao, G. Oskam, P.C. Searson, J.M. Stipkala, T.A. Heimer, F. Farzad, G.J. Meyer, *J. Phys. Chem.* 99 (1995) 11974.
- [21] I. Mora-Seró, J. Bisquert, *Nano Lett.* 3 (2003) 945.
- [22] B.C. O'Regan, F. Lenzmann, *J. Phys. Chem. B* 108 (2000) 4342.